

# The axisymmetric frictional receding contact of a layer pressed against a half-space by a point force

J.P. Lopes<sup>a,\*</sup>, D.A. Hills<sup>a</sup>

<sup>a</sup>*Department of Engineering Science, University of Oxford,  
Parks Road, Oxford OX1 3PJ, United Kingdom*

---

## Abstract

This paper uses a distribution of ring dislocations to find the solution for the frictional axisymmetric receding contact of a semi-infinite layer pressed against a half-space by a point force. The frictional behaviour between the surfaces of the layer and the half-space is modelled via Coulomb friction. The problem is fully characterized by the coefficient of friction between the interfaces. For a realistic coefficient of friction and finite load, the contact will always be partially open and partially slipping, even if there is no friction. It is shown that the interfacial tractions are proportional to the applied load while the contact area is independent of it. The transition from the unloaded to loaded configuration is discontinuous.

*Keywords:* Axisymmetric, Receding Contact, Ring dislocations

---

## 1. Introduction

Receding contacts are those where the application of a normal load causes a reduction in the size of the contact. In some problems, for example that of an over-sized pin shrink fitted into a hole in a plate have the property that the contact contracts smoothly as the applied load is gradually increased [1], but in others the contact ‘snaps’ to the final size on application of the normal load. So, for example, if the pin just referred to was mathematically of precisely the same size as the hole in which it is journalled, this property would be observed.

In machines or structures with carefully fitted parts, receding contacts are more likely to appear than advancing contacts, because of the opening of gaps between the individual parts as they distort under application of loads. Despite its importance, the literature in receding contacts was often limited to cases where there is no friction between the bodies [2, 3, 4]. More recently, Ahn and Barber [5] studied a frictional receding contact between an elastic block and a rigid substrate under cyclic loading.

Further examples include the simple, plane problem of a layer resting on a frictional, elastically similar half-plane, and with a normal line load gradually applied [6]. This

---

\*Corresponding author

*Email addresses:* jhonatan.dapontelopes@eng.ox.ac.uk (J.P. Lopes), david.hills@eng.ox.ac.uk (D.A. Hills)

*Preprint submitted to Elsevier*

*April 17, 2019*

problem is the axisymmetric equivalent, where we have a layer resting on a frictional, elastically similar half-space, and a normal point load applied. The problem is so fundamental in character that it is worth studying to learn its general properties. If the thickness of the layer is  $a$  then, from St Venant's principle, if pressure is applied over a small disk of radius  $\rho$  ( $\rho \ll a$ ) the results to be found may be expected to apply. Qualitatively, we would expect the axisymmetric problem to have much in common with the plane problem, but with one major distinction – in the plane problem the lifted-off layer, being free of stress becomes straight at points remote from the contact, and the separation from the half-plane becomes infinitely great at infinitely remote distances. In the axisymmetric case this is inhibited by the development of circumferential ( $\sigma_{\theta\theta}$ ) stress so that the surface layer has a decreasing gradient which falls smoothly at remote points.

As well as its fundamental nature the solution to be presented may be expected to have relevance to bolted plates. In reality the bolt load is spread over a washer which distributes pressure over a finite disk, as mentioned above, and the bolt must pass through a hole, of course, in both layer and half-space but, nevertheless, this idealisation may be expected to show a lot of the key properties for the bolted problem.

This paper proposes the study of the frictional axisymmetric receding contact of a homogeneous infinite layer of thickness  $a$ , Poisson's ratio  $\nu$  and modulus of rigidity  $\mu$ , pressed against an elastically similar half-space  $z \geq a$  by a point force applied to the layer's axis of symmetry (Figure 1). This represents a 'fundamental' axisymmetric receding contact problem, with only one characteristic length (the layer's thickness  $a$ ). The only independent parameter in this problem is the coefficient of friction between the layer and the half-space.

The objective of this study is to find the solution to the proposed problem using ring dislocations to introduce corrections to the stresses in the contact interface as a distribution of strain nuclei. First, we assume that the contact is in a fully closed and stuck configuration. Then, dislocation densities are applied to correct the stresses when this condition is violated.

## 2. Adhered Solution

We start our analysis by assuming that the applied force induces normal and shear tractions at the layer/half-space interface such that the contact remains closed and stuck throughout this region, i.e. the contact pressure is compressive everywhere and the shear traction is limited by Coulomb friction. Following this assumption, the state of stress in the bodies is equivalent to a half-space  $z \geq 0$  under the same loading. In the cylindrical coordinate set shown in Figure 1, the tractions  $\tilde{\sigma}_{iz}(r, z)$ ,  $i = r, z$  arising on any radial cut ( $z = \text{constant}$  surface) are given by [7]:

$$\tilde{\sigma}_{zz}(r, z) = -\frac{3P}{2\pi} \left\{ \frac{z^3}{(r^2 + z^2)^{5/2}} \right\} \quad (1)$$

$$\tilde{\sigma}_{rz}(r, z) = -\frac{3P}{2\pi} \left\{ \frac{r z^2}{(r^2 + z^2)^{5/2}} \right\}. \quad (2)$$

If the contact is, indeed, fully closed and adhered, the normal  $N(r)$  and shear  $S(r)$  tractions at the layer/half-space interface are given by:

$$N(r) = \tilde{\sigma}_{zz}(r, a) \quad (3)$$

$$S(r) = \tilde{\sigma}_{rz}(r, a). \quad (4)$$

From eqs. (1) and (2), the ratio between the normal and shear tractions at the contact interface is given by:

$$\frac{S(r)}{N(r)} = \frac{\tilde{\sigma}_{rz}(r, a)}{\tilde{\sigma}_{zz}(r, a)} = \frac{r}{a}. \quad (5)$$

Analysing eq. (5), we note that as  $r \rightarrow \infty$  the shear to normal traction ratio also goes to  $\infty$ , which means that no realistic coefficient of friction would be high enough to prevent contact slip. Furthermore, as  $r \rightarrow \infty$  the contact pressure goes to zero (eq. (1)), resulting in contact opening.

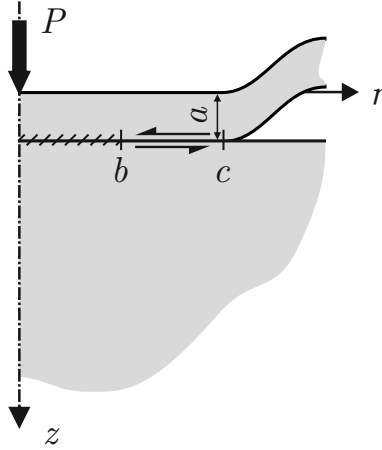


Figure 1: A layer resting in a half-space subjected to a point force.

### 3. Formulation

Since our assumption that the contact is fully stuck and closed does not hold true, the bilateral solution obtained in Section 2 is no longer valid. We expect the contact to develop regions where it is closed and partially slipping and regions where it is open as shown in Figure 1.

A modified solution can be obtained by developing expressions for the tractions at the contact interface as the sum of the adhered (bilateral) solution together with a correction in the form of an integral representation of slip and opening as a distribution of glide and climb dislocations, respectively. The dislocations needed are all ‘edge’ in character, with their Burgers vector lying in a  $\theta = \text{constant}$  plane. We emphasise that the introduction

of dislocations is used solely as a mathematical device to introduce corrections in our formulation as a distribution of strain nuclei and do not imply the introduction of physical defects in the micro-structure of the material. A more detailed explanation can be found in [8].

First, we introduce a  $b_r(\xi)$  glide dislocation loop of radius  $\xi$ , lying at a depth  $a$ . It may be formed by making a path cut along the annular disk  $\xi \leq r \leq \infty$  and sliding the surfaces by a constant amount  $b_r$ . This models contact slip and will induce the following tractions  $\hat{\sigma}_{iz}(r)$  ( $i = r, z$ ) along the same disk

$$\hat{\sigma}_{iz}(r) = G_{iz}^r(r, \xi) b_r(\xi). \quad (6)$$

The influence functions  $G_{iz}^r(r, \xi)$  are functions of Lipschitz-Hankel integrals and have extremely complicated forms. For a half-space, these are given by Paynter et al. [9] (see also [10, 11]). They are bounded ('regular') when  $i = z$  and display a Cauchy singularity when  $i = r$ .

Next, we introduce a  $b_z(\xi)$  climb dislocation loop of radius  $\xi$ , lying at a depth  $a$ . Now, the dislocation loop may be formed by making a path cut along  $\xi \leq r \leq \infty$  and inserting a disk of thickness  $b_z$ . This models contact opening and will induce the following tractions  $\hat{\sigma}_{iz}(r)$  ( $i = r, z$ ) along the same disk

$$\hat{\sigma}_{iz}(r) = G_{iz}^z(r, \xi) b_z(\xi). \quad (7)$$

Once again, the influence functions  $G_{iz}^z(r, \xi)$  are functions of Lipschitz-Hankel integrals and have extremely complicated forms. For a half-space, these are also given by Paynter et al. [9]. This time, they are bounded ('regular') when  $i = r$  and display a Cauchy singularity when  $i = z$ .

From the bilateral solution, we expect the contact to be closed and stuck from the origin to a radius  $r = b$ , closed and slipping in the region  $b \leq r \leq c$ , and open in a region extending from a radius  $c$  to infinity. Both the closure point  $c$  and stick point  $b$  are outputs of the problem (self-determining points).

The resulting normal  $N(r)$  and shear  $S(r)$  tractions along the contact interface are given by

$$N(r) = \tilde{\sigma}_{zz}(r) + \int_c^\infty G_{zz}^z(r, \xi) B_z(\xi) d\xi + \int_b^\infty G_{zz}^r(r, \xi) B_r(\xi) d\xi, \quad (8)$$

$$S(r) = \tilde{\sigma}_{rz}(r) + \int_c^\infty G_{rz}^z(r, \xi) B_z(\xi) d\xi + \int_b^\infty G_{rz}^r(r, \xi) B_r(\xi) d\xi, \quad (9)$$

where  $B_i(\xi) = db_i/d\xi$ ,  $i = r, z$  represents the dislocation density. Glide dislocations are installed over the whole of the length of the contact interface where slipping occurs, including the open portion, and climb dislocations are installed over the part of the contact interface which is open. Equations (8) and (9) form the basis of the solution and integral equations may be generated to restore conventional Signorini inequalities.

In the open region, we require the surfaces to be traction-free

$$N(r) = 0, \quad S(r) = 0, \quad c \leq r \leq \infty \quad (10)$$

whereas, in the closed, slipping region, the shearing traction is limited by friction:

$$N(r) < 0 \quad S(r) = f N(r) \quad b \leq r \leq c. \quad (11)$$

The three sets of conditions in eqs. (10) and (11) may be combined into two by making use of the Heaviside step function,  $H(\cdot)$ , giving

$$N(r) = 0 \quad c \leq r \leq \infty \quad (12)$$

$$S(r) - f H(c - r) N(r) = 0 \quad b \leq r \leq \infty. \quad (13)$$

Applying eqs. (8) and (9) to eqs. (12) and (13), gives

$$\begin{aligned} \int_b^\infty G_{zz}^r(r, \xi) B_r(\xi) d\xi + \int_c^\infty G_{zz}^z(r, \xi) B_z(\xi) d\xi \\ = -\tilde{\sigma}_{zz}(r) \quad c \leq r \leq \infty \end{aligned} \quad (14)$$

$$\begin{aligned} \int_b^\infty \left[ G_{rz}^r(r, \xi) - f H(c - r) G_{zz}^r(r, \xi) \right] B_r(\xi) d\xi + \\ \int_c^\infty \left[ G_{rz}^z(r, \xi) - f H(c - r) G_{zz}^z(r, \xi) \right] B_z(\xi) d\xi \\ = -\left[ \tilde{\sigma}_{rz}(r) - f H(c - r) \tilde{\sigma}_{zz}(r) \right] \quad b \leq r \leq \infty. \end{aligned} \quad (15)$$

Due to the nature of the functions present in eqs. (14) and (15), there is no hope of analytically inverting the integral equations. The Singular Integral Equations (SIEs) must be solved numerically, and we choose to use Gauss-Chebyshev quadrature [12]. Since there are two regions of imposition for the integral equations, two sets of quadrature points are needed. Notice that in eq. (14), the kernel  $G_{zz}^z(r, \xi)$  is Cauchy singular over the region  $c \leq r, \xi \leq \infty$  while  $G_{zz}^r(r, \xi)$  is regular. In eq. (15), the kernel  $G_{rz}^r(r, \xi)$  is Cauchy singular over the region  $b \leq r, \xi \leq \infty$  while all the other terms are regular.

The first step in solving the SIEs is to put the integrals in standard form over the interval  $[-1, 1]$ . The following transformation functions were proposed to map a normalised coordinate  $t$  to a physical coordinate  $r$ :

$$r = \frac{\lambda(t+1) + 2\hat{r}}{1-t} \quad (16)$$

$$r = \hat{r} + \lambda \log\left(\frac{2}{1-t}\right) \quad (17)$$

$$r = \hat{r} \left[ 1 + \lambda \tanh^{-1}\left(\frac{2}{1-t}\right) \right], \quad (18)$$

where  $\hat{r}$  corresponds to the lower bound of the physical interval  $[\hat{r}, \infty]$  ( $\hat{r} = \text{borc}$ ) and  $\lambda$  is a scaling parameter.

From the proposed mappings, the logarithm transformation resulted in the best description of the solution as well as the best convergence. Hence, normalising the integrals using the following substitutions:

$$u = 1 - 2 \exp\left(\frac{c - \xi}{\lambda}\right), \quad c \leq \xi \leq \infty \quad (19)$$

$$v = 1 - 2 \exp\left(\frac{c - r}{\lambda}\right), \quad c \leq r \leq \infty \quad (20)$$

$$s = 1 - 2 \exp\left(\frac{b - \xi}{\lambda}\right), \quad b \leq \xi \leq \infty \quad (21)$$

$$t = 1 - 2 \exp\left(\frac{b - r}{\lambda}\right), \quad b \leq r \leq \infty. \quad (22)$$

gives

$$\begin{aligned} & \int_{-1}^1 G_{zz}^r(v, s) B_r(s) \left(\frac{d\xi}{ds}\right) ds + \\ & \int_{-1}^1 G_{zz}^z(v, u) B_z(u) \left(\frac{d\xi}{du}\right) du \\ & = -\tilde{\sigma}_{zz}(v) \quad -1 \leq v \leq 1 \end{aligned} \quad (23)$$

$$\begin{aligned} & \int_{-1}^1 B_r(s) \left[ G_{rz}^r(t, s) + f H(\gamma) G_{zz}^r(t, s) \right] \left(\frac{d\xi}{ds}\right) ds + \\ & \int_{-1}^1 B_z(u) \left[ G_{rz}^z(t, u) + f H(\gamma) G_{zz}^z(t, u) \right] \left(\frac{d\xi}{du}\right) du \\ & = -\left[ \tilde{\sigma}_{rz}(t) + f H(\gamma) \tilde{\sigma}_{zz}(t) \right] \quad -1 \leq t \leq 1 \end{aligned} \quad (24)$$

where

$$\gamma = 1 - \frac{b}{c} + \frac{\lambda}{c} \log\left(\frac{1-t}{2}\right) \quad (25)$$

$$\frac{d\xi}{ds} = \frac{\lambda}{1-s} \quad (26)$$

$$\frac{d\xi}{du} = \frac{\lambda}{1-u}. \quad (27)$$

For the general form of the solution, both the climb and glide dislocations must be bounded at both ends of the interval. Thus, we choose

$$B_r(s) = \phi_r(s) \sqrt{1-s^2} \quad (28)$$

$$B_z(u) = \phi_z(u) \sqrt{1-u^2} \quad (29)$$

and eqs. (23) and (24) become, in normalised form,

$$\begin{aligned} & \sum_{i=1}^N \left\{ \frac{\lambda W_i}{1-s_i} \phi_r(s_i) G_{zz}^r(v_k, s_i) \right\} + \\ & \sum_{i=1}^N \left\{ \frac{\lambda X_i}{1-u_i} \phi_z(u_i) G_{zz}^z(v_k, u_i) \right\} \\ & = -\frac{2}{\pi} \tilde{\sigma}_{zz}(v_k) \quad k = 1, \dots, N+1 \end{aligned} \quad (30)$$

$$\begin{aligned} & \sum_{i=1}^N \left\{ \left[ G_{rz}^r(t_k, s_i) - f H(\gamma_k) G_{zz}^r(t_k, s_i) \right] \frac{\lambda W_i}{1-s_i} \phi_r(s_i) \right\} + \\ & \sum_{i=1}^N \left\{ \left[ G_{rz}^z(t_k, u_i) - f H(\gamma_k) G_{zz}^z(t_k, u_i) \right] \frac{\lambda X_i}{1-u_i} \phi_z(u_i) \right\} \\ & = -\frac{2}{\pi} \left[ \tilde{\sigma}_{rz}(t_k) - f H(\gamma_k) \tilde{\sigma}_{zz}(t_k) \right] \quad k = 1, \dots, N+1 \end{aligned} \quad (31)$$

where

$$\gamma_k = 1 - \frac{b}{c} + \frac{\lambda}{c} \log \left( \frac{1-t_k}{2} \right) \quad (32)$$

and the integration points  $s_i, u_i$ , collocation points  $t_k, v_k$  and weights  $W_i, X_i$  for the quadrature are given as [12]

$$s_i = u_i = \cos \left( \pi \frac{i}{N+1} \right) \quad i = 1, \dots, N \quad (33)$$

$$t_k = v_k = \cos \left( \frac{\pi}{2} \frac{2k-1}{N+1} \right) \quad i = 1, \dots, N+1 \quad (34)$$

$$W_i = X_i = \frac{1-s_i^2}{2(N+1)}. \quad (35)$$

Equations (30) and (31) form a system of  $2N+2$  equations and  $2N+2$  unknowns. These are the  $N$  values of  $\phi_r(s_i)$ ,  $N$  values of  $\phi_z(u_i)$ , the closure point  $c$  and the stick point  $b$ . Once  $\phi_r$  and  $\phi_z$  are known, the stresses at a point  $(r, z)$  can be found by the discrete versions of eqs. (8) and (9)

$$N(v) = \tilde{\sigma}_{zz}(v) + \sum_{i=1}^N \left\{ \frac{\lambda W_i}{1-s_i} \phi_r(s_i) G_{zz}^r(v, s_i) \right\} + \sum_{i=1}^N \left\{ \frac{\lambda X_i}{1-u_i} \phi_z(u_i) G_{zz}^z(v, u_i) \right\} \quad (36)$$

$$S(t) = \tilde{\sigma}_{rz}(t) + \sum_{i=1}^N \left\{ \frac{\lambda W_i}{1-s_i} \phi_r(s_i) G_{rz}^r(t, s_i) \right\} + \sum_{i=1}^N \left\{ \frac{\lambda X_i}{1-u_i} \phi_z(u_i) G_{rz}^z(t, u_i) \right\}. \quad (37)$$

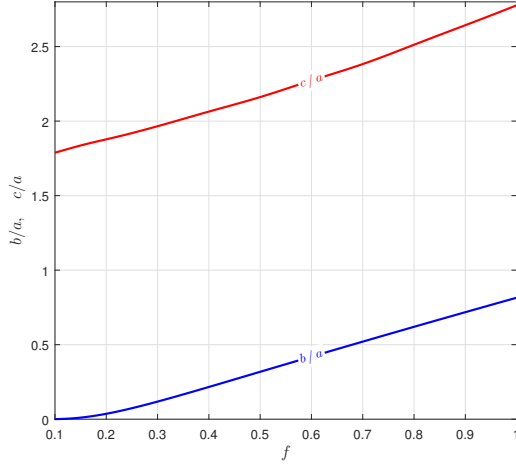


Figure 2: Normalised closure point  $c/a$  and stick point  $b/a$  as a function of the coefficient of friction.

Finally, the axial dislocation density  $B_z$  is related to the axial displacement of the contact  $u_z(r)$  through the following relationship [8]:

$$B_z(r) = -\frac{du_z(r)}{dr}. \quad (38)$$

Thus,  $u_z(r)$  can be found by integration:

$$u_z(r) = -\int_c^r B_z(\xi) d\xi. \quad (39)$$

#### 4. Results

The problem was coded up using the numerical processor MATLAB. Due to the semi-infinite nature of the integrals and, consequently, of the mapping functions, the problem is highly non-linear and obtaining a convergent solution is not trivial. First, due to the unknown length dimensions there are two additional collocation equations which need to be satisfied and which enable the values of  $b/a$  and  $c/a$  to be found. In practice, we guess values of the lengths  $b/a$  and  $c/a$  to be found and omit the central equations corresponding to  $k = N/2 + 1$  from the  $N + 1$  generated for each dislocation in eqs. (30) and (31). The column vectors of  $\phi_r$  and  $\phi_z$  are found. The omitted equations are then evaluated and residues are taken as the difference between the left and the right-hand sides of eqs. (30) and (31) for  $k = N/2 + 1$ . A programme is then used to find the values of  $b/a$  and  $c/a$  that result in the residuals being as close to zero as numerically possible.

Convergence is dependent on obtaining adequate values of quadrature points  $N$  and the scaling parameter  $\lambda$ . For the present solution, convergence was obtained for  $N = 150$  and  $\lambda = 8a$ , i.e. changes in the stresses,  $b/a$  and  $c/a$  were negligible when  $N$  was



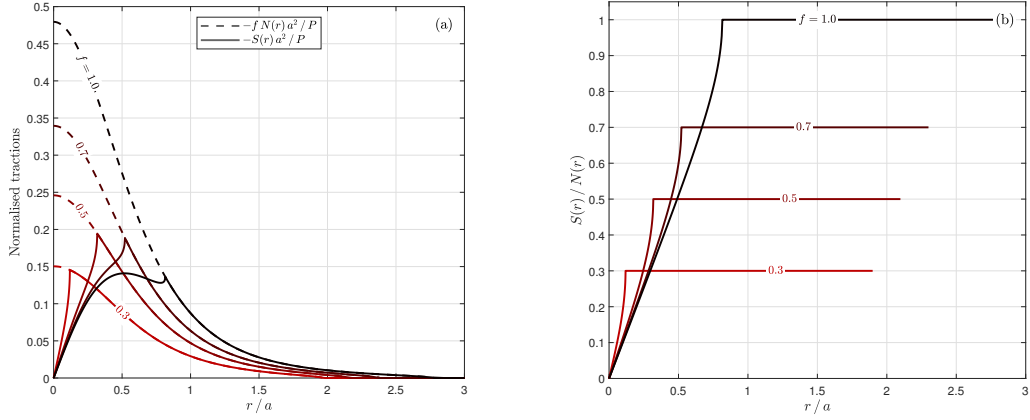


Figure 3: Traction in the contact interface. (a) Normalised contact pressure and shear stress. (b) Ratio between shear and normal stresses.

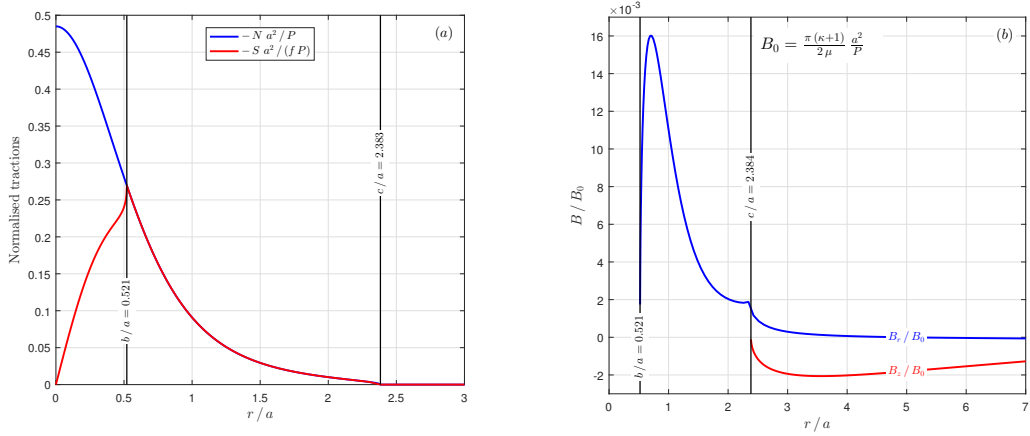


Figure 4: Results for  $f = 0.7$  at the contact interface. (a) Normalised tractions. (b) Normalised dislocation densities.

increased beyond 150 and  $\lambda$  varied slightly around  $8a$ . All results present in this paper are for  $\nu = 0.3$ .

Figure 2 shows the stick and opening points normalised with respect to the layer's thickness as a function of the coefficient of friction. As  $f$  increases, both  $b/a$  and  $c/a$  increase as well, resulting in the contact area becoming larger. This is followed by an increase in the stick zone, characterized by its radius ( $b/a$ ) becoming larger. However, the size of the slip zone is practically insensitive to the variation of the coefficient of friction, corresponding to an annulus of width  $\approx 1.8a$  for  $0.2 \leq f \leq 1.0$ . This behaviour was also observed in the equivalent plane receding contact problem of a layer subjected to a line loading [6]. On the other hand, when  $f$  is small ( $f \leq 0.2$ ),  $b \rightarrow 0$  as  $f$  decreases resulting in the stick region collapsing to a point, and the decrease in  $c/a$  results in a smaller slip zone.

Consider, now, the the contact pressure and shear stress normalised by the reference

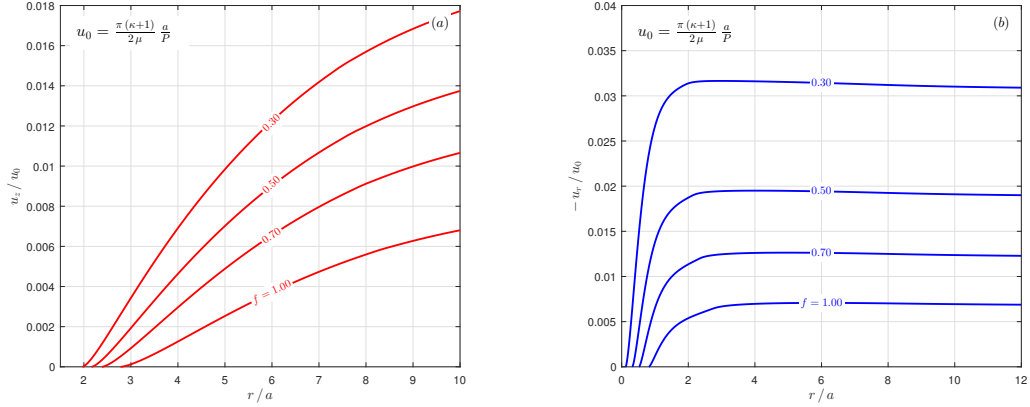


Figure 5: Normalised displacements at the contact interface. (a) Axial displacement. (b) Radial displacement.

stress  $\sigma_0 = P / a^2$  for different coefficients of friction (Figure 3). Note that the stresses are proportional to the applied pressure. The contact size, however, is independent of it and varies only with the coefficient of friction. Therefore, for any increment of load the contact ‘snaps’ from the undeformed unloaded condition to the deformed configuration, which means that, as expected, the contact area changes discontinuously from an infinite size when unloaded to a finite size upon applying any increment of load [13, 14]. For  $f = 1.0$ , even though the shear stress seems to have a peak inside the stick zone, we can see from Figure 3(b) that the ratio between  $S(r)$  and  $N(r)$  is still less than  $f$ , i.e. the slip condition is not violated.

Another property of this problem is that since the bilateral stresses in eqs. (1) and (2) are independent of the Poisson’s ratio, so does the stresses in our solution. Therefore, the tractions at the contact surface are independent of  $\nu$  and, consequently, so are the points of stick and opening. The only independent parameter in the problem is, indeed, the coefficient of friction between the interfaces.

Figure 4 shows the normalised tractions and dislocations densities for a sample coefficient of friction ( $f = 0.7$ ). Note that the radial dislocation  $B_r(r)$  goes to zero at both ends of the interval and is, therefore, bounded-bounded, as imposed in the solution. Also, since  $B_r(r)$  models contact slip, it has a maximum inside the region  $b \leq r \leq c$ , where slip occurs. The axial dislocation  $B_z$  also tends to zero as  $r$  becomes larger, but decays slower than the radial dislocation. Also, while the shear stress distribution varies significantly with respect to the coefficient of friction, the pressure distribution only changes slightly as  $f$  varies.

Figure 5 shows the normalised displacements at the contact interface for different values of  $f$  ( $\nu = 0.3$ ). In the equivalent plane receding contact problem, as the load is applied the normal contact displacement ‘snaps’ to a straight line, corresponding to a constant angle [6]. In this problem, however, the presence of a non-zero hoop strain  $\epsilon_\theta$  makes the normal contact displacement present a logarithmic curvature. As the coefficient of friction increases, it is noted that the contact opening becomes smaller.

Finally, due to the symmetry of the problem, the contact is in partial slip even for  $f = 0$ . Note from eq. (5) that when  $r = 0$ ,  $S(r)/N(r) = 0$ , which means that the point

$(r, z) = (0, a)$  needs no friction to be stuck.

## 5. Conclusions

The contact properties and tractions were obtained for a receding contact between a layer subjected to a point force and an elastically similar half-space. It was shown that the problem is fully characterised by the coefficient of friction between interfaces. For a realistic coefficient of friction, the contact will always be partially open and partially slipping, even if there is no friction.

In addition, it was shown that, as expected, the interfacial tractions are proportional to the applied load while the contact area is independent of it and changes discontinuously from the unloaded to loaded configuration with the application of an incremental load. Also, the stresses at the contact interface are independent of Poisson's ratio.

With regards to the contact area, for  $0.2 \leq f \leq 1.0$ , it was shown that an increase in the coefficient of friction results in an increase in the stick zone but no significant variance in the size of the slip annulus. Finally, due to the presence of a non-zero hoop strain, the contact opening presents a logarithmic curvature.

## Acknowledgements

D. H. thanks Rolls-Royce PLC and the EPSRC for the support under the Prosperity-Partnership Grant/ Cornerstone: Mechanical Engineering Science to Enable AeroPropulsion Futures [Grant Ref: EP/R004951/1]. J. L. gratefully acknowledges the financial support of Christ Church Oxford, Rolls Royce PLC and Coordenação de Aperfeiçoamento de Pessoal de Nível Superior - CAPES.

## References

- [1] M. Ciavarella, P. Decuzzi, The state of stress induced by the plane frictionless cylindrical contact. i. the case of elastic similarity, *International Journal of Solids and Structures* 38 (26-27) (2001) 4507–4523.
- [2] L. Keer, J. Dundurs, K. Tsai, Problems involving a receding contact between a layer and a half space, *Journal of Applied Mechanics* 39 (4) (1972) 1115–1120.
- [3] K. Tsai, J. Dundurs, L. Keer, Elastic layer pressed against a half space, *Journal of Applied Mechanics* 41 (3) (1974) 703–707.
- [4] S. El-Borgi, R. Abdelmoula, L. Keer, A receding contact plane problem between a functionally graded layer and a homogeneous substrate, *International Journal of Solids and Structures* 43 (3-4) (2006) 658–674.
- [5] Y. J. Ahn, J. Barber, Response of frictional receding contact problems to cyclic loading, *International Journal of Mechanical Sciences* 50 (10-11) (2008) 1519–1525.
- [6] T. Chaise, R. Paynter, D. Hills, Contact analysis of a semi-infinite strip pressed onto a half plane by a line force, *International Journal of Mechanical Sciences* 81 (2014) 60–64.
- [7] S. Timoshenko, J. N. Goodier, *Theory of Elasticity*, Vol. 49, 1986.
- [8] D. Hills, P. Kelly, D. Dai, A. Korsunsky, *Solution of crack problems: the distributed dislocation technique*, Vol. 44 of *Solid Mechanics and Its Applications*, Springer Netherlands, Dordrecht, 2013.
- [9] R. Paynter, D. Hills, The effect of path cut on Somigliana ring dislocations in a half-space, *International Journal of Solids and Structures* 46 (2) (2009) 412–432. doi:10.1016/j.ijsolstr.2008.09.001.
- [10] R. Paynter, D. Hills, A. Korsunsky, The effect of path cut on Somigliana ring dislocation elastic fields, *International Journal of Solids and Structures* 44 (2) (2007) 6653–6677.
- [11] J. Lopes, D. Hills, Ring cracks at the surface of a half-space, *Engineering Fracture Mechanics* 194 (2018) 105–116.

- [12] F. Erdogan, G. D. Gupta, T. Cook, Numerical solution of singular integral equations, in: Methods of analysis and solutions of crack problems, 1973, pp. 368–425.
- [13] J. Dundurs, Properties of elastic bodies in contact, The Mechanics of the Contact between Deformable bodies (1975) 54–66.
- [14] J. Dundurs, M. Stippes, Role of elastic constants in certain contact problems, Journal of Applied Mechanics 37 (4) (1970) 965–970.
- [15] G. Eason, B. Noble, I. N. Sneddon, On certain integrals of Lipschitz-Hankel type involving products of Bessel functions, Philosophical Transactions of the Royal Society of London A: Mathematical, Physical and Engineering Sciences 247 (935) (1955) 529–551.

## Appendix A. State of stress induced by circular edge dislocation loops

### Appendix A.1. Axial dislocation

Consider a climb axial dislocation loop of radius  $a$  put at a depth  $d$  and being observed at a position  $(r, z)$  in a cylindrical coordinate system, with a Burgers vector component  $b_z$ . The stress fields at a position  $(r, z)$  are given by

$$\sigma_{iz}^z(r, z) = G_{iz}^z(r, z, d) b_z(a) \quad i = r, z. \quad (\text{A.1})$$

The influence functions  $G_{iz}^z(\rho, \zeta, \delta)$  ( $i = r, z$ ) for the glide dislocation in a half-space are given as [9]:

$$G_{zz}^z(\rho, \zeta, \delta) = \frac{2\mu}{a(\kappa + 1)} \left[ -J_{1,0;1} + I_{1,0;1} - (\zeta - \delta) J_{1,0;2} - (\zeta + \delta) I_{1,0;2} + 2\zeta\delta I_{1,0;3} \right] \quad (\text{A.2})$$

$$G_{rz}^z(\rho, \zeta, \delta) = \frac{2\mu}{a(\kappa + 1)} \left[ -(\zeta - \delta) J_{1,1;2} + (\zeta - \delta) I_{1,1;2} - 2\zeta\delta I_{1,1;3} \right] \quad (\text{A.3})$$

where  $\rho$ ,  $\zeta$  and  $\delta$  are the normalised coordinates, given as

$$\rho = r/a, \quad \zeta = z/a, \quad \delta = d/a, \quad (\text{A.4})$$

$\mu$  is the modulus of rigidity and  $\kappa$  is the Kolosov's constant.

### Appendix A.2. Radial dislocation

The radial dislocation is not of Volterra kind and, thus, is path-cut dependent. In this paper, an ‘outside disk’ path cut is used [9]. This path cut can be formed by inserting a disk of material at a depth  $z = d$ , from  $r = a$  to  $r = \infty$ , displacing the material by the same amount  $b_r$  (thickness of the disk). The stress fields at a position  $(r, z)$  are given by

$$\sigma_{iz}^r(r, z) = G_{iz}^r(r, z, d) b_r(a) \quad i = r, z. \quad (\text{A.5})$$

The influence functions  $G_{iz}^r(\rho, \zeta, \delta)$  ( $i = r, z$ ) for the glide dislocation in a half-space are given as [9]:

$$G_{zz}^r(\rho, \zeta, \delta) = \frac{2\mu}{a(\kappa + 1)} \left[ -(\zeta - \delta) J_{0,0;2} + (\zeta - \delta) I_{0,0;2} + 2\zeta\delta I_{0,0;3} \right] \quad (\text{A.6})$$

$$G_{rz}^r(\rho, \zeta, \delta) = \frac{2\mu}{a(\kappa + 1)} \left[ J_{0,1;1} - I_{0,1;1} - (\zeta - \delta) J_{0,1;2} + (\zeta + \delta) I_{0,1;2} - 2\zeta\delta I_{0,1;3} \right] \quad (\text{A.7})$$

### Appendix A.3. Lipschitz-Hankel integrals

In the influence functions, the terms  $J_{n,p;q}$  and  $I_{n,p;q}$  represent Lipschitz-Hankel integrals. The standard definition for these functions is as an integral of the product of Bessel functions ( $J_i(\cdot)$ ), an exponential term and a power term. Using normalised coordinate variables, it is given as [15]

$$P_{\mu,\nu;\lambda}(\rho, \zeta) = \int_0^\infty J_\mu(t) J_\nu(\rho t) e^{-\zeta t} t^\lambda dt. \quad (\text{A.8})$$

In the kernels, the follow definition is applied:

$$J_{n,p;q} = P_{n,p;q}(\rho, \zeta - \delta) \quad (\text{A.9})$$

$$I_{n,p;q} = P_{n,p;q}(\rho, -\zeta - \delta) \quad (\text{A.10})$$

The Lipschitz-Hankel integrals needed in the kernels are given by Paynter et al. [10, 9].